Journal of Engineering Physics and Thermophysics, Vol. 75, No. 2, 2002

TESTING OF A MULTIBLOCK ALGORITHM OF CALCULATION OF NONSTATIONARY LAMINAR SEPARATING FLOWS

S. A. Isaev, A. G. Sudakov, P. A. Baranov, and N. A. Kudryavtsev

UDC 512.517.2

Based on a comparative analysis of results of numerical and physical modeling of nonstationary laminar separating flows of an incompressible fluid, a factorized calculational algorithm on the basis of multiblock intersecting grids is verified.

1. It is well known that most of the occurring hydrodynamic and thermophysical processes are nonstationary and require nonstationary calculational algorithms for their prediction. In recent publications [1–3], numerical modeling of separating flows developing in the near wake of a circular cylinder and a bar in flow and also in a tunnel with a moving burning railroad car has been considered within the framework of the strategy which is based on the application of multiblock intersecting calculational grids and an implicit factorized procedure. It seems expedient to carry out a methodological investigation aimed at testing the indicated multiblock algorithm of calculation of laminar nonstationary flows with separation of the flow. For this purpose we have selected test problems on the process of establishment of flow of an incompressible viscous fluid about a circular cylinder for a Reynolds number of 40 and the initial stages of development of the near wake of a circular cylinder for Reynolds numbers of 500 and 5000. We carry out a comparative analysis of the calculation results and the available experimental data and results of calculating separating flows by other numerical methods.

2. As is well known, in many if not in most cases of practical importance the streamlined body is characterized by the presence of flow-forming elements whose linear dimensions are much smaller than the characteristic dimension of the body. Construction of multiblock grids to calculate the flow about such structures is frequently impossible or leads to an unacceptably large number of calculational nodes. At the same time, any topologically complex calculational region can be subdivided into a number of regions of simple geometry which allow the construction of grids of ordinary form (rectangular, O-shaped, and S-shaped grids). The subregions usually adjoin at certain interfaces determined in advance for which the equation of motion of the fluid must also be solved. The latter circumstance restricts somewhat the possibilities of such an approach, since it requires that the nodes of the calculational grid of superposed regions coincide along the line of joining.

An alternative can be the approach adopted in this work; to calculate the flow this approach uses a set of partially intersecting regions in each of which its own independent grid is constructed. The equations of motion are solved separately in each region. Information is exchanged between the regions in the zones of their mutual intersection with the use of interpolation dependences that relate the values of the variables at the nodes of different regions.

Consideration is given to the laminar flow of a Newtonian viscous incompressible fluid in the absence of mass forces. The flow is described by Navier–Stokes equations that are written in vector form as

$$\frac{\partial \mathbf{V}}{\partial t} = -\nabla (\mathbf{V}\,\mathbf{V}) + \nabla [\nu (\nabla \mathbf{V} + \nabla \mathbf{V}^T)] - \nabla p \,. \tag{1}$$

The equation of transfer of momentum is supplemented with the continuity equation

$$\nabla \mathbf{V} = 0 \,. \tag{2}$$

Equations (1) and (2) are written in dimensionless form. The coordinates are made dimensionless by means of the characteristic dimension L, the velocity components are made dimensionless by means of a certain characteristic

Academy of Civil Aviation, St. Petersburg, Russia; email: isaev@SI3612.spb.edu. Translated from Inzhenerno-Fizicheskii Zhurnal, Vol. 75, No. 2, pp. 28–35, March–April, 2002. Original article submitted April 27, 2001.

 1062-0125/02/7502-0300$27.00

velocity U_0, the pressure is made dimensionless by means of the double velocity head ρU_0^2, and the viscosity is made dimensionless by means of $U_0 L$.

The boundaries of the regions of flow calculated in practice have a rather complex geometry; to describe it correctly one must use curvilinear and in the general case nonorthogonal coordinate systems. The use of curvilinear coordinates produces known difficulties which are related to the appearance of terms containing Christoffel symbols. The presence of these terms, very sensitive to the skewness and nonuniformity of the grid cells, can lead to a loss in the exactness of solutions. Furthermore, in this case the equations of motion acquire a nonconservative form. One way of solving this problem is considered in [4], where the form of representation of the equations of motion for covariant components of the velocity vector without Christoffel symbols is given. We note that the adoption of the approach of [4] can lead to errors for coarse and nonuniform grids. This is caused by the fact that in constructing a difference analog by discretization of differential equations the balance of forces is properly computed not for the actual faces of the control volume but for the "average" ones (which are peculiar for each direction) whose orientation and size are determined at the center of the volume. The errors of such a replacement are especially perceptible when, for example, polar grids with a significant nonuniformity in the radial direction are used. Because of this, discretization of the equations of motion will be carried out based on the control-volume method that guarantees obtaining a rigorously conservative form of difference equations, as has been done, in particular, in [5].

Let us introduce two coordinate systems into consideration, i.e., a Cartesian system x, y and an arbitrary curvilinear coordinate system x^1, x^2. We will assume that the nondegenerate transformation converting the curvilinear region in the physical space to a rectangular region in the space of generalized coordinates exists. To construct the difference scheme we integrate Eqs. (1) and (2) over the separated control volume P with the faces e, w, n, and s and pass from the volume integrals to surface ones.

It is generally assumed that the nonstationary and source terms are constant in the control volume. It is also adopted that the basis vectors, dependent variables, and their derivatives are constant within the face of the control volume and are equal to the values computed at the center of the face. In representing the subsequent expressions, it is taken into account that the strain-rate tensor can be represented in the form of the dyads of the dual-basis vectors and of the derivatives of the velocity vector along the corresponding curvilinear coordinates

$$(\nabla \mathbf{V} + \nabla \mathbf{V}^T) = \mathbf{e}^k \frac{\partial \mathbf{V}}{\partial x^k} + \frac{\partial \mathbf{V}}{\partial x^k} \mathbf{e}^k,$$

while the scalar gradient, by definition, is written as

$$\nabla k = \mathbf{e}^k \frac{\partial k}{\partial x^k}.$$

Taking the steps along the curvilinear coordinates x^k to be equal to 1 and passing from the integrals to summation with respect to the faces of the control volume, we obtain the following system of equations:

$$\sqrt{g_P} \frac{\partial \mathbf{V}_P}{\partial t} = -\sum_{e,w,n,s} (\Delta \mathbf{s}\, \mathbf{V})\, \tilde{\mathbf{V}} + \sum_{e,w,n,s} \nu\, \Delta \mathbf{s} \left(\mathbf{e}^k \frac{\partial \mathbf{V}}{\partial x^k} + \frac{\partial \mathbf{V}}{\partial x^k} \mathbf{e}^k \right) - \sum_{e,w,n,s} p\, \Delta \mathbf{s}. \tag{3}$$

In these expressions, $\Delta \mathbf{s}$ is the vector of the area of the corresponding face of the calculational grid coinciding with the vector of the external normal in direction and determined as

$$\Delta \mathbf{s}_e = \mathbf{e}_e^1 \sqrt{g_e}; \quad \Delta \mathbf{s}_w = \mathbf{e}_w^1 \sqrt{g_w}; \quad \Delta \mathbf{s}_n = \mathbf{e}_n^2 \sqrt{g_n}; \quad \Delta \mathbf{s}_s = \mathbf{e}_s^2 \sqrt{g_s}.$$

The parameters denoted as $\tilde{\mathbf{V}}$ represent quantities determined at the centers of the faces; the method of computation of these quantities depends on the selected scheme of convective transfer.

The obtained expressions (3) determine the balance between the convective-diffusive flows through the faces of the control volume and the nonstationary and source terms determined at its center. When the control-volume

method is used it is precisely these equations that are the object of discretization carried out in constructing the finite-difference analog of the initial equations.

In the system of equations (3), special emphasis should be placed on the first equation describing the balance of surface and bulk forces. To construct the difference scheme one must convert this vector equation into a system of scalar equations, having selected the basis (natural, dual, or Cartesian) and hence the type of dependent variable in advance. Thereafter the system of scalar equations is easily obtained by multiplying the vector equation by the vectors of the corresponding basis which are computed at the center of the control volume.

As far as the selection of the basis employed is concerned, we note that this problem is closely connected with selection of the calculational template of layout of the variables. Thus, when a staggered grid is used the employment of the Cartesian components of the velocity vector is practically impossible in the regions of a complex configuration since arbitrarily oriented velocity components up to tangential ones and not the components normal to them can turn out to be prescribed on the faces. In this case, the employment of either covariant velocity components, as has been done in [4], or contravariant components is the standard solution. An alternative can be the use of a centered template, widely employed at present, in which all the variables are located at the center of the control volume. In this version, the employment of co- or contravariant components loses its meaning in many respects and even decreases the efficiency of program codes because of the need for continuous conversion of some components to others in the process of solution. At the same time, it is expedient to use the Cartesian components for the following reasons (in addition to simplicity and clarity): first, in this case the flows through the common face of two adjacent cells can be computed once and employed subsequently without additional recalculation to determine the coefficients of the equations and the source terms in both cells, which significantly improves the efficiency of computations; the second circumstance is connected with the necessity of determining the values of the velocities at the centers of the faces and of the template edges, i.e., of employing interpolation of the velocities. Whereas for the Cartesian components this procedure is quite obvious, in interpolation of, for example, covariant velocities to correctly reconstruct other velocity components (Cartesian or contravariant ones) from the found values one must also necessarily interpolate the basis vectors at the point of interpolation. Otherwise, the test of a "uniform" flow can be disturbed. Interpolation of the basis vectors leads to the fact that the actual dimensions and orientation of the faces of the control volume will be replaced by the averaged ones, which can lead to a loss in the exactness of the solution, especially on curvilinear nonuniform grids.

Here, the centered template is employed in combination with selection of the Cartesian components of the velocity vector as dependent variables.

The metric coefficients are calculated in advance (details are presented in [6]).

The positions of the centers of the control-volume edge are assumed to be prescribed. Let us assume that they are determined as the average values of the coordinates of angular points. From expressions (3) it follows that we must find the values of the following quantities for program implementation:

$V^1_{e,w}$ and $V^2_{n,s}$, contravariant velocity components at the centers of the faces which are computed according to the metric determined at the same points;

$(\mathbf{e}^k)_{P,e,w,n,s}$ and $(\mathbf{e}_k)_{P,e,w,n,s}$, k = 1, 2, vectors of the dual and natural bases at the center of the template and at the centers of the faces;

$\sqrt{g_{P,e,w,n,s}}$, determinant of the metric tensor at the same points.

We write the final expressions for the quantities involved in the three-dimensional equation of motion, taking the step along the curvilinear coordinate to be 1:

$$\mathbf{e}_1 = \mathbf{i}\frac{\partial x}{\partial x^1} + \mathbf{j}\frac{\partial y}{\partial x^1}; \quad \mathbf{e}_2 = \mathbf{i}\frac{\partial x}{\partial x^2} + \mathbf{j}\frac{\partial y}{\partial x^2},$$

where **i** and **j** are the unit vectors of the Cartesian coordinate system.

In the difference expression for the central point, we have

$$(\mathbf{e}_1)_P = \mathbf{i}\frac{x_E - x_W}{2} + \mathbf{j}\frac{y_E - y_W}{2}, \quad (\mathbf{e}_2)_P = \mathbf{i}\frac{x_N - x_S}{2} + \mathbf{j}\frac{y_N - y_S}{2}.$$

For the *e*-face, for example, we have

$$(\mathbf{e}_1)_e = \mathbf{i}\,(x_E - x_P) + \mathbf{j}\,(y_E - y_P)\,, \quad (\mathbf{e}_2)_e = \mathbf{i}\,(x_{en} - x_{es}) + \mathbf{j}\,(y_{en} - y_{es})\,.$$

The covariant components of the metric tensor are

$$g_{ik} = \mathbf{e}_i\,\mathbf{e}_k = e_{i_x}\,e_{k_x} + e_{i_y}\,e_{k_y}\,.$$

The determinant of the metric tensor is

$$\sqrt{g} = e_{1_x}\,e_{2_y} - e_{2_x}\,e_{1_y}\,.$$

Passage from the vectors of the natural basis to those of the dual basis is determined by the expressions

$$\mathbf{e}^1 = \frac{\mathbf{i}\,e_{2_y} - \mathbf{j}\,e_{2_x}}{\sqrt{g}}\,, \quad \mathbf{e}^2 = \frac{\mathbf{i}\,e_{1_y} - \mathbf{j}\,e_{1_x}}{\sqrt{g}}\,.$$

We also give expressions to recalculate the velocities. For the contravariant components at the centers of the faces, they have the form

$$V_e^i = \mathbf{V}_e\,(\mathbf{e}^i)_e = (V_x)_e\,(e_x^1)_e + (V_y)_e\,(e_y^1)_e\,.$$

In constructing the finite-difference algorithm, we employ schemes written in increments in the quantities sought, i.e., for the equation of the form

$$L\,(\Phi) = F$$

the difference approximation will be represented as

$$L_1^h\,(\delta\Phi) = F^h - L^h\,(\Phi^h)\,,$$

where the superscript h means approximation on a certain grid, while the difference operator L_1^h can differ from the operator L^h. Such an approach makes it possible to construct efficient schemes with a high rate of convergence of the iterative process, which is attained primarily by the employment of the lowered order of approximation of the convective terms in the operator L_1^h as compared to the operator L^h. Furthermore, it becomes possible to introduce artificial damping in the operator L_1^h, which results in a stabilized process of computations [7].

The derivatives of the form $\partial\Phi/\partial x^k$, $\Phi = \mathbf{V}$ involved in the system of equations (4) are replaced by their difference analogs, which are computed at the centers of the faces as follows:

$$\left.\frac{\partial\Phi}{\partial x^1}\right|_e = \Phi_E - \Phi_P\,; \quad \left.\frac{\partial\Phi}{\partial x^2}\right|_e = \Phi_{en} - \Phi_{es}\,;$$

$$\left.\frac{\partial\Phi}{\partial x^1}\right|_w = \Phi_P - \Phi_W\,; \quad \left.\frac{\partial\Phi}{\partial x^2}\right|_w = \Phi_{wn} - \Phi_{ws}\,;$$

$$\left.\frac{\partial\Phi}{\partial x^1}\right|_n = \Phi_{en} - \Phi_{wn}\,; \quad \left.\frac{\partial\Phi}{\partial x^2}\right|_n = \Phi_N - \Phi_P\,;$$

$$\left.\frac{\partial \Phi}{\partial x^1}\right|_s = \Phi_{es} - \Phi_{ws}\,; \quad \left.\frac{\partial \Phi}{\partial x^2}\right|_s = \Phi_P - \Phi_S\,.$$

In the expressions for the total convective flows of the form $\sum_{e,w,n,t} (\Delta \mathbf{s}\mathbf{V})\tilde{\Phi}$, the quantity $(\Delta \mathbf{s}\mathbf{V})$ determines the flow rate of the fluid through the corresponding face; the transfer rate is determined at the center of the face by linear interpolation from the values at the nearest nodes. The parameters denoted as $\tilde{\mathbf{V}}$ represent quantities which are also determined at the centers of the faces and are computed in accordance with the selected scheme of convective transfer. In this work, we consider the most popular scheme of approximation of convective terms, i.e., the Leonard scheme of quadratic interpolation [7]. We represent the scheme for an arbitrary face, having explicitly separated the part which corresponds to the upwind scheme with one-sided differences:

$$\tilde{\Phi} = \Phi_L - \mathrm{COR}\,(\Phi_R - \Phi_L, \Phi_L - \Phi_{LL}) \quad \text{for} \quad (\Delta \mathbf{s}\,\mathbf{V}) > 0\,;$$

$$\tilde{\Phi} = \Phi_R - \mathrm{COR}\,(\Phi_L - \Phi_R, \Phi_R - \Phi_{RR}) \quad \text{for} \quad (\Delta \mathbf{s}\,\mathbf{V}) < 0\,,$$

where the function COR (x_1, x_2) is determined as follows: COR $(x_1, x_2) = -0.375x_1 - 0.125x_2$ for the Leonard scheme.

On the basis of Eq. (3) and taking into account the above relations, we write the entire implicit difference scheme in increments; this scheme is designed to solve the equations of transfer of momentum [7]

$$a_P \delta\,\mathbf{V}_P = a_E \delta\,\mathbf{V}_E + a_W \delta\,\mathbf{V}_W + a_N \delta\,\mathbf{V}_N + a_S \delta\,\mathbf{V}_S + \mathbf{b}_P\,, \tag{4}$$

where

$$a_E = \max\,[-\Delta \mathbf{s}_e\,\mathbf{V}_e, 0] + \mathrm{OTL}\,\nu\,\Delta \mathbf{s}_e\,\mathbf{e}_e^1 = \max\,[-\sqrt{g_e}\,V_e^1, 0] + \mathrm{OTL}\nu\,\sqrt{g_e}\,g_e^{11}\,,$$

$$a_W = \max\,[-\Delta \mathbf{s}_w\,\mathbf{V}_w, 0] + \mathrm{OTL}\,\nu\,\Delta \mathbf{s}_w\,\mathbf{e}_w^1 = \max\,[-\sqrt{g_w}\,V_w^1, 0] + \mathrm{OTL}\nu\,\sqrt{g_w}\,g_w^{11}\,,$$

$$a_N = \max\,[-\Delta \mathbf{s}_n\,\mathbf{V}_n, 0] + \mathrm{OTL}\,\nu\,\Delta \mathbf{s}_n\,\mathbf{e}_n^2 = \max\,[-\sqrt{g_n}\,V_n^2, 0] + \mathrm{OTL}\nu\,\sqrt{g_n}\,g_n^{22}\,,$$

$$a_S = \max\,[-\Delta \mathbf{s}_s\,\mathbf{V}_s, 0] + \mathrm{OTL}\,\nu\,\Delta \mathbf{s}_s\,\mathbf{e}_s^2 = \max\,[-\sqrt{g_s}\,V_s^2, 0] + \mathrm{OTL}\nu\,\sqrt{g_s}\,g_s^{22}\,,$$

$$a_P = a_E + a_W + a_N + a_S + \frac{\sqrt{g_P}}{\Delta t}\,,$$

$$\mathbf{b}_P = -\sum_{e,w,n,s} (\Delta\,\mathbf{s}\,\mathbf{V})\,\tilde{\mathbf{V}} + \sum_{e,w,n,s} \nu\,\Delta\,\mathbf{s}\left(\mathbf{e}^k \frac{\partial\,\mathbf{V}}{\partial x^k} + \frac{\partial\,\mathbf{V}}{\partial x^k}\,\mathbf{e}^k\right) - \sum_{e,w,n,s} p\,\Delta\,\mathbf{s} - \sqrt{g_P}\,\frac{\mathbf{V}_P - \mathbf{V}_P^{\mathrm{old}}}{\Delta t}\,.$$

We note that the coefficients of the difference scheme which correspond to the convective term of the equation are computed using the upwind scheme with one-sided differences, i.e., the single scheme making it possible to reliably obtain the diagonal predominance of the matrix of the coefficients. Furthermore, following [7], we have introduced the scheme parameter $\mathrm{OTL} > 1$ into the diffusion part of the coefficients; this parameter enables us to improve the stability of the calculational procedure owing to suppression of nonphysical high-frequency oscillations.

To more accurately describe the nonstationary processes, following [8], in approximating the nonstationary term it is expedient to employ the Peyret three-point scheme of second order of time approximation

$$\sqrt{g_P}\,\frac{\partial\,\mathbf{V}_P}{\partial t} = \sqrt{g_P}\left(1.5\,\mathbf{V}_P^{n+1} - 2\mathbf{V}_P^n + 0.5\,\mathbf{V}_P^{n-1}\right)/\Delta t\,.$$

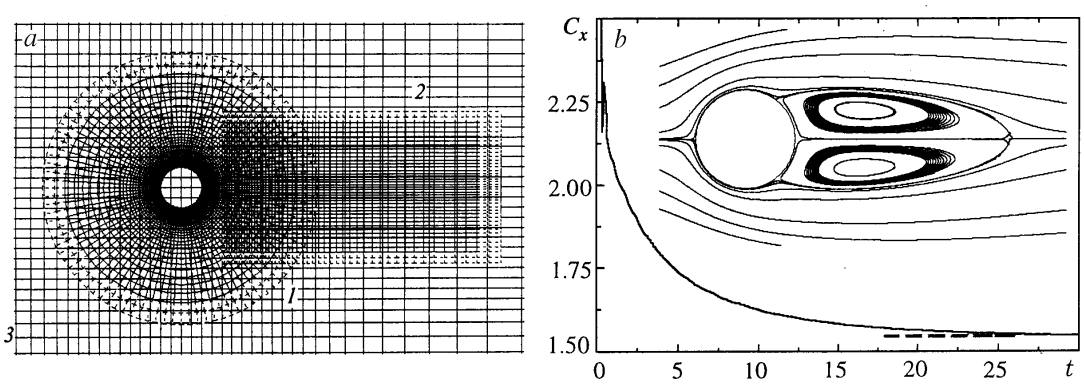

Fig. 1. Fragment of the multiblock grid (a) for calculating flow about a circular cylinder [1) cylindrical grid adjacent to the cylinder; 2) rectangular grid in the near wake; 3) external rectangular grid] and the coefficient of drag as a function of the time for Re = 40 (b). The dashed line on the plot and the pattern of flow about the cylinder correspond to the stationary regime.

Equations (3) and the difference scheme (4) constructed based on them enable us to obtain the solution of the nonstationary problem of flow or the solution of the stationary problem by the method of establishment. In the case where the nonstationary effects are of no interest it is more expedient to employ schemes constructed based on the stationary equations of transfer. We will employ the implicit difference schemes written in the E-factor formulation [7]

$$a_P \delta \mathbf{V}_P = a_E \delta \mathbf{V}_E + a_W \delta \mathbf{V}_W + a_N \delta \mathbf{V}_N + a_S \delta \mathbf{V}_S + \mathbf{b}_P , \tag{5}$$

$$a_P = \left(1 + \frac{1}{\mathrm{E}}\right)\left(a_E + a_W + a_N + a_S + \frac{\sqrt{g_P}}{\Delta t}\right),$$

$$\mathbf{b}_P = -\sum_{e,w,n,s} (\Delta \mathbf{s}\, \mathbf{V})\, \tilde{\mathbf{V}} + \sum_{e,w,n,s} \nu\, \Delta \mathbf{s} \left(\mathbf{e}^k \frac{\partial \mathbf{V}}{\partial x^k} + \frac{\partial \mathbf{V}}{\partial x^k} \mathbf{e}^k \right) - \sum_{e,w,n,s} p\, \Delta \mathbf{s} .$$

Noteworthy is the presence of the term $\sqrt{g_P}/\Delta t$ in the expression for a_P. In this case Δt acts as the scheme parameter making it possible to improve the stability of numerical solution by decreasing the convergence rate and not as the time step.

The calculational procedure at each time step is based on the concept of splitting by physical processes which is implemented in the procedure of pressure correction [7, 9]. The characteristic features of the iteration algorithm are determination, at the predictor step, of the preliminary velocity components for frozen pressure fields and subsequent correction of the pressure on the basis of the solution of the continuity equation with corrections of the velocity field. The computational process is constructed in such a manner that one predictor step accounts for several local iteration steps in the block of pressure correction. The calculational procedure also involves the interpolation block of determination of dependent variables in the zones of overlapping of the subregions. Transfer of the values between the intersecting grids is carried out within the framework of multiblock grid strategy using a nonconservative linear interpolation whose details are presented in [10].

3. Laminar flow of an incompressible viscous fluid about a circular cylinder has long been a test problem for testing the developed calculational algorithms. In the 1930s, Thom solved the problem on the stationary regime of flow near a circular cylinder for Re = 40 on arithmometer-like devices, while in the 1960s Fromm demonstrated the von Kármán vortex trail developing behind a rectangular cylinder for Reynolds numbers of about 100. Despite the great number of works on a numerical analysis of flow about a cylinder, they do not include investigations performed within the framework of a multiblock multigrid strategy.

In this work, special emphasis is placed on the transient regimes of flow about a circular cylinder which is characterized by the symmetric structure of the vortex flow in a near wake. For a moderate Reynolds number of 40

TABLE 1. Comparison of the Results of Calculation of Laminar Flow of an Incompressible Viscous Fluid about a Cylinder for a Reynolds Number of 40

Type of grid	Number of cells	C_{xp}	C_{xf}	C_x	C_{pf}	C_{pb}	X_r
$\Delta t = 0.05$	11751	1.013	0.535	1.547	1.138	–0.532	2.13
$\Delta t = 0.1$	11751	1.011	0.536	1.547	1.137	–0.531	2.15
$\Delta t = 0.2$	11751	1.009	0.537	1.546	1.135	–0.532	2.16
$\Delta t = 0.5$	11751	1.010	0.542	1.551	1.135	–0.532	2.16
$\Delta t \to \infty$	11751	1.009	0.531	1.540	1.142	–0.523	2.17
$\Delta t \to \infty$ ○-type	17600	0.995	0.525	1.527	1.144	–0.505	2.22

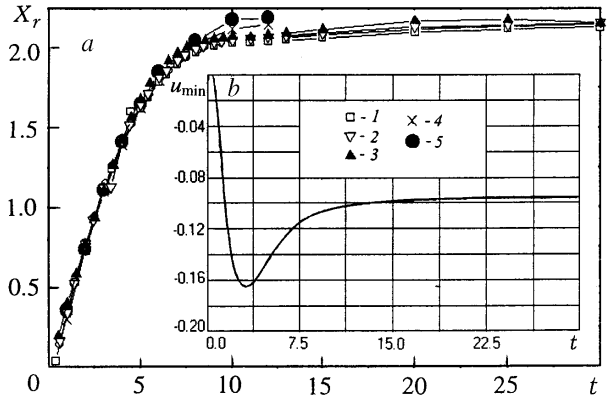

Fig. 2. Length of the separation zone behind the cylinder X_r (a) and minimum velocity of the return flow in the near wake $u_{\min}$ (b) vs. time (solid curves correspond to Δt = 0.05). The calculated data 1) Δt = 0.1, 2) 0.2, and 3) 0.5 are applied for comparison, as well as the calculated data 4 (Δt = 0.1) and the experimental data 5 taken from [8].

such a regime lasts until the flow pattern is established, while for Re > 500 the existence of the regime is confined to the initial, the so-called accelerating, period of flow about the cylinder.

The calculations are performed on a set of cylindrical and rectangular grids (Fig. 1a). We note that all the linear dimensions are referred to the diameter of the cylinder. An annular wall region of size 0.2 containing 15 × 100 cells is adjacent to the contour of the cylinder. The wall step of the grid is selected to be 0.05. Next, the external ring of size 2 containing 20 × 100 cells is butt-joined to the wall region. The cylindrical grids are built into the external rectangular grid with dimensions 49 × 60 which contains 71 × 71 nonuniformly distributed nodes with a minimum step of 0.2. To more correctly reproduce the characteristics of the near wake behind the cylinder a 5.5 × 3 rectangular grid region containing 50 × 40 cells with a minimum step of the grid of 0.05 is placed behind the cylinder at a distance of 0.8 from the center.

In integrating with respect to time, we employ the implicit procedure with approximation of the time derivative according to the Peyret scheme of second order of accuracy.

The boundary conditions were prescribed in the ordinary manner: the parameters of a uniform flow with zero and excess pressure were taken at the inlet boundary of the external rectangular region and "soft" boundary conditions were taken at the remaining boundaries. The initial conditions corresponded to the state of occurrence of a sudden motion of the cylinder or of impact of the flow against its surface. The adhesion conditions were prescribed on the contour of the body. The velocity of the incoming flow was selected as the dimensionless scale.

Figures 1–4 and Table 1 give some of the numerical results obtained.

The plot (Fig. 1b) of the drag coefficient of the circular cylinder versus time (for a time step of 0.05) shows the monotone asymptotic character of this dependence for the Reynolds number Re = 40. This asymptotics is similar in value to the drag of the circular cylinder in the case of the stationary regime of flow about it (see Table 1).

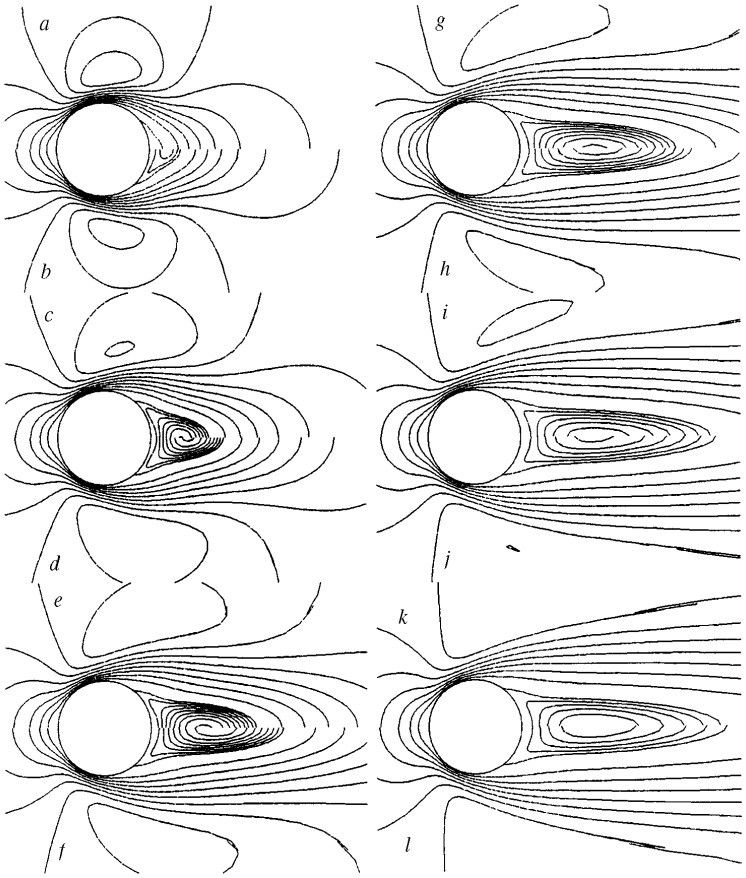

Fig. 3. Evolution of the pattern of flow about a circular cylinder for Re = 40 from the sudden beginning of the motion; the isoline fields of the longitudinal velocity component are shown at the following instants of time: a) t = 0.6, b) 1.05, c) 1.65, d) 2.05, e) 3.05, f) 4.05, g) 5, h) 6, i) 8, j) 10, k) 15, and l) 20, applied with a step of 0.02 in the region of negative values and with a step of 0.15 in the region of positive values of u.

Table 1 gives data for the integral characteristics of nearly stationary (at t = 30) or stationary flow about the cylinder which have been calculated using different time steps, algorithms, and grids. The first five lines contain the data of calculations according to the proposed multiblock technique. The results of calculations of stationary flow about the cylinder on a monoblock cylindrical grid of O-type for a minimum step of 0.002 near the wall and a distance to the external boundary of the region of 40 are presented in the sixth line [11]. In addition, it should be noted that from the experimental data of Apelt C_x = 1.413 for Re = 40 and the length of the circulation zone behind the cylinder is X_r = 2.2.

The calculated asymptotic integral characteristics of the nonstationary flow about the cylinder for different time steps are similar to the corresponding characteristics of the stationary flow and to the data of physical experiment.

In Fig. 2a, the practical coincidence of the results of calculations of the evolution of the separation zone in the near wake behind the cylinder, which have been performed for different time steps, is noteworthy. In dynamics, they are in good agreement with the available data of calculations on monoblock grids and with the data of physical experiments [8].

It is significant that the given dependences of C_x and X_r on time have a monotone character; however, time changes of the local characteristics, in particular, of the maximum velocity of return flow in the near wake, can have extrema (Fig. 2b). Thus, a local minimum of velocity nearly twice as high as the velocity in the stationary regime of flow about the cylinder is realized at t = 3.15.

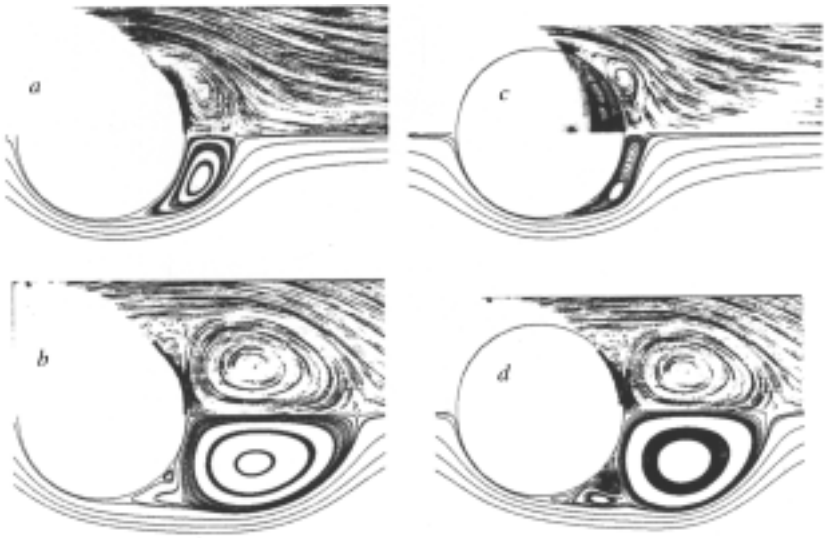

Fig. 4. Comparison of the calculated and experimental (taken from the Van Dyke Atlas [12]) patterns of flow about a circular cylinder for Reynolds numbers of 500 (a and b) and 5000 (c and d) at the instant of time t = 1 (a and c) and 3 (b and d).

The reason for such behavior of the local parameters of flow is analyzed in Fig. 3, where the evolution of flow about the cylinder is shown beginning from the nearly initial instant of time (t = 0.6) to a practically established pattern (t = 20). It should be noted that the results presented in Fig. 2b and Fig. 3 are obtained with the calculational step Δt = 0.05.

As is seen from Fig. 3, the "impact" period of flow about the cylinder is excluded from consideration. We must admit that its influence on the entire process is not very substantial, i.e., different degrees of resolution of the initial period have no marked consequences. Even the smoothing of this phase in gradual acceleration of the cylinder does not change the characteristics of the subsequent stages of the process.

The analysis of Figs. 2a and 3 shows that the dynamics of the process of flow about the cylinder is the highest at the initial instants t = 1–4 when the length of the separation zone in the near wake increases with the highest rate and the velocity of the return flow attains its maximum in absolute value. The external flow becomes much weaker.

The final stage of development of the process is characterized by the gradual establishment of the flow, relative damping of it in the separation zone, and a certain elongation of this zone. On the whole, the greatest changes in this phase are observed in the period t = 5–10.

Figure 4 illustrates the influence of the viscosity on the initial phase of the process of flow about a circular cylinder. The increase in the Reynolds number leads to the effect of "wrinkling" of the separation zone behind the cylinder as compared to the low values of Re. We can state a certain retardation of the development of the process with decrease in the diffusion influence on separating flow.

Just as in the case of investigations of circulation flow in a square cavity with a moving boundary [7], the regions of secondary separation and reattachment of the flow occur in the separation zone in the wake behind the cylinder with increase in the Reynolds number. As is seen in Fig. 4b and d, the increase in Re leads to the progressive convection in the separation zone, to intensification of the flow in the zones of secondary vortices, and even to the occurrence of tertiary vortices.

The comparative analysis of the results of calculation according to the multiblock technique and of the presented data of physical experiments on visualization of the patterns of nonstationary flow about a circular cylinder shows quite an acceptable accuracy of numerical calculations and illustrates the testing of the algorithm presented.

This work was carried out with support from the Russian Foundation for Basic Research under project Nos. 00-02-81045, 02-02-81035, 99-01-00722, and 02-01-01160.

NOTATION

t, time; Δt, time step; x, y, Cartesian coordinates; x^1, x^2, arbitrary curvilinear coordinate system; $\mathbf{e}^k$, units vectors of the curvilinear coordinate system; $\mathbf{V}$, velocity vector; u, Cartesian velocity component; p, pressure; Φ, generalized variable; ν, molecular viscosity; Re, Reynolds number; a and b, coefficients in the difference equations; C_x, C_{xp}, and C_{xf}, coefficients of drag, pressure resistance, and friction; C_{pf} and C_{pb}, coefficients of pressure at the leading and trailing critical points of the cylinder; X_r, length of the separation zone in the near wake behind the cylinder. Subscripts and superscripts: P, E, W, N, and S, modes of the template; e, w, n, and s, centers of the faces of the calculational cell; min, minimum value; L, R, LL, and RR, parameters at the centers of the cells adjacent to the selected face ($LL = L - 1$; $RR = R + 1$); n, number of the time step.

REFERENCES

1. P. A. Baranov, S. A. Isaev, and A. G. Sudakov, *Mekh. Zhidk. Gaza*, No. 2, 68–74 (2000).
2. P. A. Baranov, S. A. Isaev, and A. E. Usachov, *Inzh.-Fiz. Zh.*, **73**, No. 3, 606–613 (2000).
3. P. A. Baranov, A. D. Golikov, S. A. Isaev, et al., *Inzh.-Fiz. Zh.*, **73**, No. 5, 918–921 (2000).
4. Yu. E. Karyakin, V. E. Karyakin, and O. G. Martynenko, *Numerical Modeling of Laminar Flows of a Viscous Fluid in Arbitrarily Shaped Channels*, Preprint No. 1 of the Academic Scientific Complex "A. V. Luikov Heat and Mass Transfer Institute" [in Russian], Minsk (1991).
5. P. A. Baranov, V. L. Zhdanov, and A. G. Sudakov, *Numerical Calculation of the Nonstationary Flow about a Cylinder with Induced Vorticity in a Near Wake*, Preprint No. 5 of the Academic Scientific Complex "A. V. Luikov Heat and Mass Transfer Institute" [in Russian], Minsk (1998).
6. S. A. Isaev, P. A. Baranov, N. N. Luchko, et al., *Numerical Modeling of the Separating Flow of an Incompressible Fluid in Square and Cubic Cavities with a Moving Boundary*, Preprint No. 7 of the Academic Scientific Complex "A. V. Luikov Heat and Mass Transfer Institute" [in Russian], Minsk (1999).
7. I. A. Belov, S. A. Isaev, and V. A. Korobkov, *Problems and Methods of Calculation of Separating Flows of Incompressible Fluids* [in Russian], Leningrad (1989).
8. I. A. Belov and N. A. Kudryavtsev, *Heat Transfer and Resistance of Tube Banks* [in Russian], Leningrad (1987).
9. S. A. Isaev, N. A. Kudryavtsev, and A. G. Sudakov, *Inzh.-Fiz. Zh.*, **71**, No. 4, 618–631 (1998).
10. 9. S. A. Isaev, A. I. Leont'ev, P. A. Baranov, et al., *Inzh.-Fiz. Zh.*, **74**, No. 2, 62–67 (2001).
11. P. A. Baranov, S. A. Isaev, Yu. S. Prigorodov, et al., *Izv. Vyssh. Uchebn. Zaved., Aviats. Tekh.*, No. 3, 30–35 (1999).
12. M. Van Dyke, *An Album of Fluid Motion* [Russian translation], Moscow (1986).